Soft Matter

PAPER

View Article Online
View Journal | View Issue

Cite this: *Soft Matter*, 2025, **21**, 6814

Surface functional group dependent enthalpic and entropic contributions to molecular adsorption on colloidal microplastics

Ikechukwu Kanu, Amrit Ojha, Kalie Adams, Jacob Brooks and Mahamud Subir *

Molecular interaction with micro- and nano-plastics (MNPs) is an important chemical process that dictates the fate and transport of organic contaminants, and that of MNPs, within the aquatic environment. In this study, adsorption of cationic, anionic, and neutrally charged organic molecules from aqueous solution to model microplastics (MPs) is presented. Second harmonic generation, an interfacial selective laser-based technique that allows *in situ* measurements of adsorption isotherms, has been used. Polystyrene (PS) and polymethyl methacrylate (PMMA) microplastic particles with distinct charge characteristics were chosen. PS MPs investigated include distinct surface functional groups such as $-OSO_3$, $-COOH$, mixed $-NH_2/-COOH$, and amidine. Thus, the effect of different types of electrostatic interactions on adsorption have been analyzed. Comparison of adsorption Gibbs free energy for these MPs reveals that Coulombic attraction is important for spontaneous adsorption. However, distribution of water at the interfacial region, and functional group dependent interactions determine the magnitude of binding strengths. Entropic (ΔS_{ads}) and enthalpic (ΔH_{ads}) contributions to spontaneous adsorption have been determined by analyzing temperature-dependent adsorption isotherms. We show that ΔH_{ads} and ΔS_{ads} are dependent on the interfacial chemical composition of MPs and are not constant with respect to temperature. Although of varying degrees, MPs studied show an increase in entropy upon adsorption of organic molecules. These findings hint at a plausible influence of hair-like structure, common in polymeric soft matter, on the adsorption mechanism. This systematic study thus underscores unique colloidal features of the plastic/aqueous interface that are critical in adsorption of organic molecules by microplastics.

Received 12th May 2025,
Accepted 9th August 2025

DOI: 10.1039/d5sm00488h

rsc.li/soft-matter-journal

Introduction

Microplastics are increasingly being detected in our rivers, lakes, oceans, deep sea, and the terrestrial environment.[1–7] Considered as contaminants of emerging concerns, micro- and nano-plastics (MNPs) vary extensively with respect to their chemical composition. Microplastics are defined[6,8] as any kind of plastic fragments, beads, and fibres with a diameter in the range of 100 nm to <5 mm;[9–11] whereas, nano-plastics are less than 100 nm.[10,11] Because of their polymeric nature, MNPs are considered a form of soft matter. Given their size range, MNPs exhibit colloidal behaviour; that is, their interfacial structure and charge properties become important in understanding how these particles interact with their surroundings. Indeed, in a recent perspective,[12] it has been proposed that "adopting a view of microplastics as a colloid provides a holistic framework that connects their physical properties and surface chemistries with observations of their dynamics in the environment."

From the colloidal viewpoint, MNPs in the nano- and microscopic range provides a large surface area to volume ratio. Thus, colloidal MNPs serve as a transport vector for many organic contaminants.[13–17] In the aquatic environment, these small organic pollutants can also be charged or neutral. Once adsorbed onto the surface of MNPs, they can be transported within the aquatic environment by physical mechanisms, and exhibit altered chemical reactivity. Recent literature[18–20] exploring interactions of organic compounds with microplastics has highlighted that in-depth studies on the adsorption behaviour of organic pollutants on MNPs are limited and systematic studies on the mechanism of adsorption are warranted. The wide range of MNP types, chemical composition and surface charge properties necessitates a systematic investigation on the influence of MNP interfacial properties on molecular adsorption. Accordingly, the aim of this study has been to address new interfacial chemistry-specific questions that have emerged:

Department of Chemistry, Ball State University, Muncie, Indiana, USA.
E-mail: msubir@bsu.edu

What drives the molecular adsorption – pure charge interactions, specific interactions, or the exclusion of hydrophobic compounds from water? Is the adsorption, if any, entropically or enthalpically driven? Elucidating these fundamental interfacial processes involving MNPs and organic molecules is vital to the understanding of how these contaminants propagate through our water systems and impact the environment.

There is a variety of polymers found in microplastics detected in the environment. Examples include polyethylene, polypropylene, polyvinyl chloride, polycarbonate polymethyl methacrylate, and more. In recent studies, both polystyrene (PS) and polymethyl methacrylate (PMMA) has been highlighted for their negative impact with respect to their toxicity and availability in the environment.[21–24] PS polymer, which contains aromatic rings, is prevalent in many of these MNPs.[25,26] Polystyrene, $(-C_8H_8)_n$, a thermoplastic with rigid chains, is found in styrofoam products, packaging materials, and many other economical plastic materials.[22,27] In contrast, polymethyl methacrylate (PMMA), also known as acrylic, is a transparent thermoplastic and is often used as glass substitute for lenses, windows (*e.g.*, plexiglass), and cosmetics. It consists of methyl ester $(-C_5H_8O_2)_n$ functional groups. In this study, particles with core compositions of polystyrene and polymethyl methacrylate have been chosen because these chemicals are common in microplastics. However, it is important to note that while the core of the MNPs may be represented by their polymer structures described above, their surfaces can contain different functional groups such as –COOH and $-NH_2$. These species are ionizable. Even hydrophobic microplastics often carry surface charges in the aquatic medium.[10,28] Polymeric chains of MNPs are also likely to extend out into the aqueous phase, a characteristic of interfacial structure of soft matter. Thus, different types of interactions are possible when adsorption of organic compounds onto colloidal MNPs is considered.

Similarly, small organic compounds in the aquatic environment exhibit hydrophobic/hydrophilic characteristics.[29] These contaminants can be charged or neutral, and are also subject to hydrophobic and Coulombic interactions. The diversity in functional groups in these compounds can also allow specific interactions such as hydrogen bonding or pi–pi interactions. For this study, the main objectives are to (1) deduce if favourable molecule–particle interaction is dominated by attraction between opposite charges or if van der Waals forces are sufficient for adsorption on MNPs and (2) explain if a spontaneous adsorption is enthalpically or entropically driven and whether it is dependent on specific surface functional groups. Thus, this study examines the surface chemistry (interfacial charge and chemical composition) on the adsorption of charged and neutral organic compounds.

An important criterion for a systematic adsorption study involving colloids is that the experiments be done *in situ*, without perturbing the colloidal suspension. Separation techniques are not suitable for MNPs of similar density as water because gravimetric centrifugation can induce aggregation and perturbation of the adsorption equilibrium. For this reason, we have utilized interfacial specific technique known as second harmonic generation (SHG). Specifically, we present SHG-based molecular adsorption studies of three different—cationic, anionic, and neutral—organic compounds on six different microplastics (MPs). The MPs used are all approximately micrometre in diameter. This is to avoid size-dependent SHG scattering effect on the adsorption analysis. Four of the MPs are PS-based, varying in surface chemical compositions including, bare polystyrene (PS), sulfate (PSS), carboxyl (PSC), aliphatic amine (PSAA), and amidine (PSAm), and one composed of PMMA. To deduce thermodynamic adsorption parameters (ΔH_{ads} and ΔS_{ads}) temperature-dependent adsorption isotherms have been collected for adsorptions characterized by Langmurian model. Interestingly, our results demonstrate that not only charge but the soft interfacial structure of MPs and bound water molecules play a pivotal role on molecular adsorption.

Experimental

Materials and methods

Chemicals and materials. The organic dyes of different charge properties, *trans*-4-[4-(dimethylamino)styryl]-1-methylpyridinium iodide (DSMPI, dye content 98%, No. 336408), and naphthol yellow S (NYS, $\geq$99.0%, Catalog No. 49547) were purchased from Sigma-Aldrich. Coumarin 314 (C314, 99%, No. AC405621000, ACROS Organics), was obtained from Fisher Scientific. Polystyrene (PS, Lot # 642745) microsphere was obtained from Polysciences, Inc. According to the manufacturer, these monodispersed polystyrene microspheres contain a slight anionic charge from sulfate ester. Polystyrene sulfate (PSS, Lot# 2897860), carboxylate (PSC, Lot# 2427068), zwitterionic polystyrene aliphatic amine (PSAA, Lot# 2040155) and polystyrene amidine (PSAm, Lot# 2178691) were obtained from ThermoFisher Scientific. PSAA is zwitterionic because it includes a high density of amine and carboxyl groups on the surface. Product specification suggests that the parking area per amino group is 74 $Å^2$ per NH_2 and that of carboxyl group is 1349 $Å^2$ per COOH. Non-functionalized colloidal poly-methyl methacrylate (PMMA, Batch# 22328) was purchased from Alpha Nanotech, Inc. Surface functionalized PMMA particles are not commercially available. All chemicals were stored as suggested by the manufacturer and characterized using UV-vis spectrometer (UV 2600i, Shimadzu) and ZetaSizer ZS (Malvern Analytic), a dynamic light scattering (DLS) technique, prior to use. The DLS instrument allows determination of size (hydrodynamic diameter) and zeta (ζ) potential of the MPs. Smoluchowski approximation has been used. In a typical measurement, three runs were performed, and the average size or ζ-potential and corresponding standard deviations were recorded. The value of the size reported is based on peak intensity.

A digital analytical balance was employed for precise weighing of the organic compounds. Millipore water, with a resistivity of 18.2 MΩ cm was used for all sample preparation. The MP suspensions exhibited a similar pH as that of the neutral Millipore water. To ensure precision in sample preparation, Fisher-brand sterile disposable standard pipets were used for

dispersing and preparing the solutions. The dye solutions were prepared at varying concentrations in single-use clear 30 mL vials. Dye solutions were prepared through systematic serial dilution methodology. Serological transfer pipets were used for solution preparation. The particle number density, determined based on their size, W/V ratio, and polymer density, was provided by the manufacturer. This concentrated suspension was diluted in a 30 mL clean vial with Millipore water to obtain the MP stock solution with a density of 2×10^8 particles per mL for our experiments. These stock solutions were stored in a dark place at room temperature for no longer than one week. Glassware was thoroughly cleaned using Aqua Regia (3 : 1 mixture of HCl and HNO_3 acids) solution. For the adsorption studies, all dyes and MP samples were prepared in clean glass vials. The final mixtures of the dye and the particle were prepared by 50/50 dilution of the stock dye solution and MP suspensions. For instance, to prepare a 10 mL mixture of 10 μM of DSMPI dye in the presence of 1×10^8 mL^{-1} PSC particles, 5 mL of 20 μM DSMPI solution was mixed with 5 mL of 2×10^8 mL^{-1} PSC. Mixtures were vigorously vortexed. For SHG correction, the same stock solutions were used to prepare the reference samples of the dye and the PSC alone, at the desired concentration and number density, respectively. For the dye and MP mixtures, ample time, approximately 30 minutes, was given for an adsorption equilibrium to reach between the dye and the particle-aqueous interface. Adsorption kinetic experiments in our group have demonstrated that an adsorption equilibrium is reached within a few minutes.

Second harmonic generation. SHG is a special case of second order nonlinear spectroscopy in which two photons of the same frequency from the incoming laser beam interact with a material and produce a new photon. The resulting photon oscillates at twice the frequency of the initial photons.[30,31] The role of symmetry is critical in SHG. In centrosymmetric materials, such as bulk solutions, SHG is forbidden under the electric approximation of light–matter interaction but can occur at surfaces because these regions naturally lack inversion symmetry. For this reason, SHG has been applied to study various surfaces, including that of colloidal interfaces. The details of the SHG method in generating adsorption isotherms and obtaining information of the adsorption energetics have been described elsewhere.[32,33] In brief, the SHG intensity, I_{SHG}, is proportional to the number density (N_{ads}) of the molecules that are adsorbed on the interface (eqn (1)). This allows mapping out the adsorbate profile at the MP/aqueous interfaces by plotting I_{SHG} as a function of dye concentration. SHG is also dependent on the hyperpolarizability, $\langle\alpha^{(2)}\rangle$, averaged over molecular orientation. Thus, how the molecule is oriented may influence the strength of the SHG intensity. For instance, well-aligned molecules can yield stronger SHG signal compared to randomized dipoles.

$$I_{SHG} \propto |N_{ads}\langle\alpha^{(2)}\rangle|^2 \quad (1)$$

The SHG experiments utilized a solid-state Nd:YVO_4 (Millenia eV) to pump a Ti:Sapphire Tsunami oscillator (3941X1BB) with 70 fs pulses at a repetition rate of 80 MHz. Both lasers were purchased from Spectra Physics. The fundamental laser beam was tuned to ~800 nm and directed to a 1.0 cm quartz cuvette containing the sample. The cuvette was placed in a flash 300 temperature-controlled cuvette holder (Quantum Northwest). The colloidal suspension was stirred using a small magnetic bar and adjusted to the target temperatures of 13 °C (±0.5), 22 °C, 35 °C, and 50 °C, each within 0.2 °C. The power at the sample was set at ~450 mW and monitored to be within ±2% throughout the experiment. The beam was passed through a red filter and focused using a lens with a focal length of 5.0 cm. The polarization of the incident beam was varied using a half-wave plate (WPH10M-808, Thorlabs). The polarizations perpendicular and parallel to the laser table are defined as vertical (V) and horizontal (H), respectively. The scattered signal was then collimated by a second lens and the second harmonic field was passed through a blue filter to block the residual fundamental beam. The beam is passed through an analyzer set to detect V-polarized light. The SHG signal is further guided to a monochromator (Acton SP2500, Princeton Instruments) for better spectral separation. A photomultiplier tube served as a detector. The photocurrent produced by a photomultiplier tube (PMT, H11461P-01, Hamamatsu) was transmitted to a preamplifier (SR445A, Stanford Research Systems (SRS), Inc.). The amplified signal was then directed at a single photon counter (SR400, SRS, Inc.) and then processed using LabView Software. The SHG intensity in the range of 370–430 nm was collected for each sample and the peak intensity, spectra centered at the second harmonic wavelength, was used to generate adsorption isotherm. A total of five spectra per sample were collected and the peak intensities for each were averaged. The standard deviation in the intensities were used to calculate the standard error each data point.

Data processing to generate SHG-based isotherm involved correcting the raw signal for scattering loss and subtraction of hyper-Rayleigh background signal. The detailed correction procedure has been discussed previously.[32,34] In brief, the raw intensity from each sample was corrected for opacities based on Beer–Lambert law. Optical densities of the samples at both the fundamental and SHG wavelengths, as determined from UV-vis absorptions spectroscopy, have been used for this correction. Thereafter, the intensities from the corresponding dye solution and MPs alone were subtracted from the intensities of the dye-MP mixture. Two-photon fluorescence from the dyes was not observed at the second harmonic wavelength. Data analysis, including non-linear least-squares data fitting of the adsorption isotherms, was carried out using IgorPro. The fitting approach utilizes Levenberg–Marquardt algorithm to search for the minimum value of chi-square (χ^2), based on initial guesses of the coefficient values.

Results and discussion

(1) Characterization of the dye molecules and the MPs.

As alluded to in the introductory section, a critical aspect of determining thermodynamic parameters of binding at the MP surface is the ability to measure adsorption isotherms *in situ*,

without mechanical perturbation of colloidal suspension. All these organic compounds exhibit absorbance bands around 400 nm,[32] which provides resonance enhancement with the SHG wavelength in these experiments. Fig. S1 in SI shows the absorbance spectra of these compounds in aqueous solution. DLS measurement provided information on the size (hydrodynamic diameter) and charge properties of the MPs used. Fig. 1(A) shows that all the particles studied are approximately 1 μm. PMMA shows a larger standard deviation because of possible aggregation. As can be seen in Fig. 1(B), PMMA exhibits the lowest magnitude of zeta potential. Hence PMMA particles are likely to coalesce during the time window of size measurement using DLS.

Despite the different interfacial chemical compositions, PSS, PS, PSC, and PSAA, show negative ζ-potential. While the magnitude of the zeta potential depends on various factors such as the location of the slipping plane and counter ion adsorption, based on the sign, it is apparent that these particles contain excess negative charge at the interface. PSS carries negative charge due to the sulfate group and as noted in the Experimental section, PS MPs contain negative charge from sulfate ester. However, given that the extent of sulfate groups on PS particle surface is less than that of PSS, it is expected that the PS MPs are more hydrophobic than PSS. Comparing molecular adsorption onto these MPs therefore helps to distinguish the effect of hydrophobicity in the presence of the same charged species. The negative charge on PSC is due to the deprotonated COOH group. The interfacial pK_a of PSC is 5.4;[35] thus, significant amount of carboxylate ion is expected near neutral pH. For this reason, zwitterionic PSAA appears to show an excess of negative charge at its interface. The use of PSC *versus* PSAA thus highlights the effect of carboxyl group and reduced density of carboxyl group, respectively, on molecular adsorption. PSAm displays positive zetapotential because it contains positively charged amidine functional groups on the surface.

PMMA does not have any ionizable groups at its surface; however, its ζ-potential value is slightly negative. Observation of negative zeta potential on hydrophobic interfaces is not uncommon. Generation of charged interfaces *via* contact electrification, asymmetric partitioning of hydroxide ions, a collective polarization/charge transfer effect are possible mechanisms.[36–39] It is important to distinguish however that the observed negative zetapotential on PMMA is not due to a fixed charged species but likely because of an accumulation of loose and mobile ions. Thus, comparison of molecular adsorptions on the loosely bound negatively charged PMMA *versus* that of the PS, PSS, and PSC, where most of the charges are fixed, provides a critical insight into the nature of electrostatic interaction.

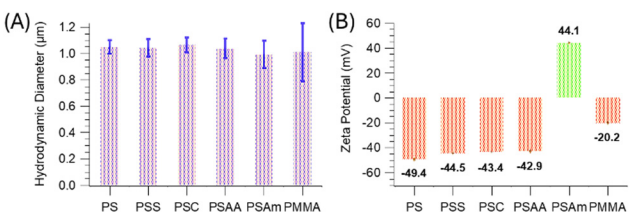

Fig. 1 Size and charge property characterization of the colloidal MPs used in this study. Hydrodynamic diameter (A) and zeta-potential (B) measured based on DLS.

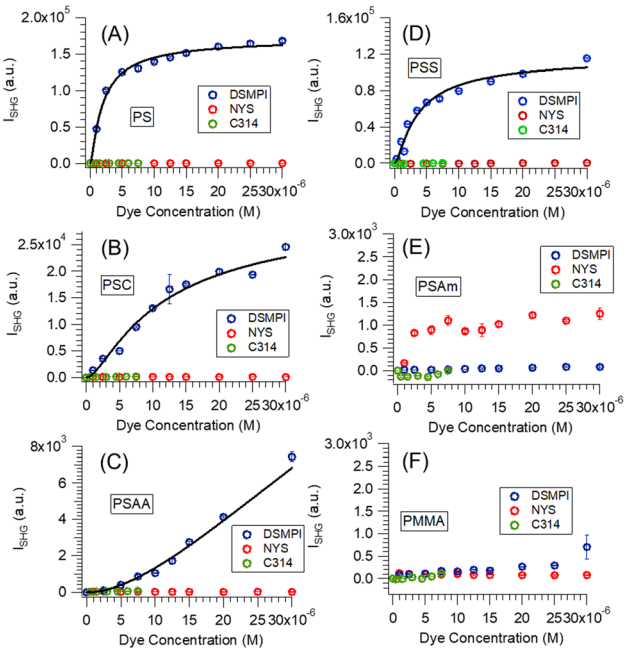

Fig. 2 SHG-based adsorption isotherms of DSMPI (blue markers), NYS (red markers), and C314 (green markers), onto MPs of different surface composition: (A) PS, (B) PSC, (C) PSAA, (D) PSS, (E) PSAm, and (F) PMMA. These data were collected at 22 °C. Markers represent experimental data, and the solid curves represent Langmurian fit to the data.

(2) Role of Coulombic interaction on molecular adsorption

We are now in position to compare the effect of charge on molecular adsorption. Fig. 2 shows a set of SHG-based adsorption isotherm collected with the cationic (DSMPI), anionic (NYS), and neutral (C314) organic molecules at 22 °C for the six different MPs studied herein. The plots show SHG intensity as a function of the concentration of the molecules in the aqueous solution. Based on eqn (1), these graphs map out the relative number density of adsorbates at the interface. A rise in the signal means adsorption is occurring and no increase in signal implies no adsorption.

The major observations are as follows:

(i) the positively charged molecule, DSMPI, adsorbs onto most of the negatively charged MPs. It adsorbs onto PS, PSC, PSAA, and PSS, all of which are expected to have fixed negative charge densities at the interface owing to the functional groups present at these MP surfaces. The adsorption isotherms generated follow a Langmuir model, which will be discussed in part 3 of the Results and discussion section. As anticipated, DSMPI does not adsorb onto positively charged PSAm due to Coulombic repulsion. Interestingly, no DSMPI adsorption is observed for PMMA even though it exhibits negative zeta potential. Recall, the chemical structure of PMMA entails hydrophobic moieties which should not produce fixed negatively charged functional groups at its interface. The source of the negative ζ-potential at the hydrophobic interface may involve mobile ions.

Thus, these results demonstrate that the nature or the origin of the interfacial charge dictates whether the adsorption of organic molecule is spontaneous. We surmise that fixed charge density at the particle/aqueous interface is necessary for organic ion to adsorb *via* Coulombic interaction.

(ii) The negatively charged NYS molecule does not adsorb to the negatively charged PS, PSS, PSC, PSAA, and PMMA MP/aqueous interfaces. Coulombic repulsion explains this behaviour. For the positively charged PSAm, a steep rise in the SHG signal at very low concentration is observed, followed by a plateau. This is a tell-tale sign of high affinity adsorption, often observed for polymeric or protein substrates.[40,41] The SHG signal is weak compared to DSMPI adsorption at the negatively charged MP surfaces. The charge on NYS is −2; thus, a greater extent of Coulomb attraction to the positively charged PSAm exists. This explains the high affinity isotherm behaviour. It does not follow a Langmurian profile. Eqn (1) shows SHG intensity scales with molecular orientation. The relatively weak SHG intensity may thus indicate that due to high affinity NYS molecules are randomized at the interface, resulting in cancellation in the generated SHG field. Yet, it is apparent from the sharp jump in signal that there is an interaction between the oppositely charged dye-MP pair.

(iii) C314, a neutral and hydrophobic molecule, does not show any increase in SHG intensity for all the particles investigated. Note, the extent of C314 concentration explored is limited by its solubility. Within the concentration range studied, C314 does not adsorb to these particles. This and along with the observations (i) and (ii), it appears that Coulomb attraction is important in driving molecular adsorption. van der Waals type interaction does not serve as a driving force for adsorption. This appears to suggest that despite the hydrophobic core of these MPs, the MP/aqueous interface is highly solvated and thereby polar. This finding is consistent with a previous study based on spectral shift which demonstrated the aqueous-particle interface of PSC to be polar.[42] Moreover, C314 has previously been shown to adsorb at the hydrophobic air/water[43] as well as the hexadecane/water nanoemulsion[32] interfaces. These chemical systems do not have trapped or strongly associated water molecules at the interfacial region. Therefore, we surmise that unlike pure Coulombic attraction, weak van der Waals interaction is not sufficient to overcome the hydrated MP layer. Thus, the neutral C314 molecules do not stick to these polymer surfaces. This finding is applicable for small hydrophobic molecules and does not imply that neutral organic compounds do not bind to microplastics. Sufficiently large hydrophobic molecules, such as long chain polymers has the potential to overcome the energetic barrier of displacing water molecules and interact *via* extended van der Waals force with the MP.

These observations raise more questions. For instance, what is the strength of binding (ΔH_{ads}) and entropy change (ΔS_{ads}) for the adsorption of charged molecules? Moreover, do they depend on the surface functional group or Coulombic interactions is the dominant mode of binding? Answering these questions require a deeper understanding of the thermodynamics of the adsorption process for the model microplastics.

(3) Mechanistic insights into molecular adsorption

To deduce the binding strength and the entropy change of adsorption, we have collected temperature dependent isotherms using DSMPI for the PS, PSS, PSC, and PSAA particles. We focused on the adsorption of the positively charged DSMPI onto MPs containing fixed negative charges because Langmurian adsorption behaviour has been observed for these interactions. SHG adsorption isotherms of these MP-DSMPI pairs have been collected and by fitting the data using the Langmuir model (see SI), the equilibrium adsorption constants (K_{ads}) were determined. In our experiments, the overall surface area of the MPs is in the order of 10^{16} Å^2 per mL of solution. Assuming full and closely packed surface coverage of the dye at saturation, the amount of dye depleted from solution upon adsorption would be sub-micromolar. That is, $c_{bulk} \gg c_{surface}$ throughout the adsorption process.[41] Thus, initial solution concentration, instead of equilibrium concentration, has been used in the Langmuir fitting. Replicates of these isotherms are shown in Fig. S2 of the SI. The Langmuir fit parameters of the isotherms are tabulated in Table S2. The adsorption Gibbs free energy is calculated using $\Delta G_{ads} = -RT \ln K_{ads}$ at each temperature. Plots of ΔG_{ads} *versus* T for each of the particle are shown in Fig. 3. The slope is related to ΔS_{ads} as follows:

$$\Delta S_{ads} = -\left(\frac{\partial \Delta G_{ads}}{\partial T}\right)_P \quad (2)$$

Rearranging eqn (3) allows calculation of ΔH_{ads}.

$$\Delta G_{ads} = \Delta H_{ads} - T\Delta S_{ads} \quad (3)$$

It is evident that for most of these particles, ΔG_{ads} is not a linear function of temperature within the range studied. This is particularly true for PS, PSC, and PSAA. This means ΔS_{ads} and ΔH_{ads} for these particles vary with temperature. Heat capacity of polystyrene is relatively constant below its glass transition temperature (T_g).[44] According to the manufacturer, T_g of polystyrene is 100–110 °C. Thus, the variation of heat capacity is not the source of the nonlinearity in ΔG_{ads} within the temperature range of this study. The implication is that there is more than

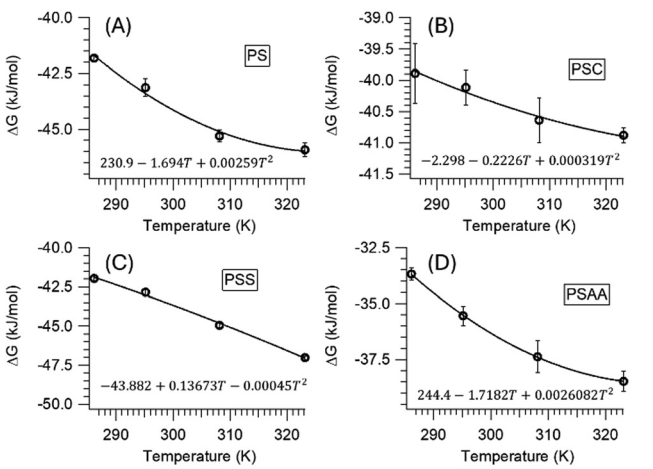

Fig. 3 Plots of ΔG_{ads} *versus* T for (A) PS, (B) PSC, (C) PSS, and (D) PSAA.

one type of interaction taking place at the interface. Since DSMPI has the same chemical form, different interactions are attributed to the compositions of the MP surface. As an example, for the PS particles, the adsorbate can not only interact with the hydrophobic polymer but also the sulfate groups. Similarly, other particles can provide both hydrophobic and hydrophilic interactions, the latter due to their polar functional groups. Given the nonlinearity, Van't Hoff equation, which assumes ΔH to be constant with temperature, is not applicable. It has been verified previously that description of the nonlinear dependence with a quadratic form is a good approximation in most cases.[45]

We have found second order (quadradic) polynomial functions to fit the data well. The functional form is provided within each graph. The fit coefficients along with residuals are tabulated in Table S1 of the SI. These coefficients are limited to the temperature range of the experimental data. The ΔS_{ads}, and ΔH_{ads} values have been calculated using eqn (2) and (3), respectively. These values, calculated for 22 °C, are reported in Table 1. Thermodynamic parameters calculated for all temperature are shown in Table S3 of the SI.

A major observation is that $\Delta S_{ads} > 0$ for the adsorption of DSMPI to these particles. The positive entropy change implies that there is an increase in randomness upon DSMPI adsorption. Generally, adsorption entails diminished degrees of motion for the adsorbates and thus a decrease in entropy. This is often the case when molecules adsorb from vapour phase to a solid substrate. However, MPs are in contact with water. Thus, an increase in entropy observed in these experiments suggests that prior to the adsorption of the organic compound, water molecules are bound to the MP surface. Adsorption of the organic molecules leads to a release of water molecules, which in turn increases disorder. Similar behaviour has been observed for molecular adsorption onto cellulose-based surfaces and biological polymer particles.[46,47] It is also observed that the magnitude of ΔS_{ads} of the hydrophobic PS and PSAA decreases significantly with increasing temperature (Fig. 4). This is consistent with the picture that water molecules are initially adsorbed at the interfacial layer. At higher temperature less water molecules are bound to the particle interface due to increased molecular motion. The change in ΔS_{ads} is steep for PS and PSAA, and gradual for PSC. For the PSS there is a slight increase in ΔS_{ads} with temperature. Clearly, the presence of significant amount of negatively charged sulfate groups affects the thermodynamics of adsorption.

For PSC and PSS, water molecules are expected to be strongly bound to the $-OSO_3^-$, $-COOH/-COO^-$ due to the abundance of fixed negative charges on these MPs. It has been shown that water molecules favour negative charges.[48] H-bonding is also possible with carboxyl functional group. Increase in temperature has a miniscule effect on the strongly bound H_2O molecules. In contrast, in the case of PS and PSAA, the sharp change in ΔS_{ads} can be explained as follows. Most of the water molecules are trapped in the hydrophobic polymer layer, which is more sensitive to temperature. As temperature increases, flexible polymer chains can protrude into the bulk water, resulting in fewer water molecules trapped at higher temperature. Thus, with increasing temperature, adsorption onto MP does not entail displacement of sufficient water molecules to cause a significant change in entropy at higher temperatures. In addition, the positive ΔS_{ads} and its variation with temperature suggest that adsorption of organic compounds to microplastics involves an exchange process. These MPs are well hydrated. This means molecules of higher affinity displace another molecule, such as water, that is already adsorbed at the interfacial region.

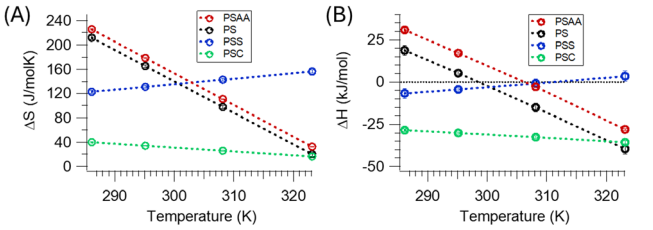

Fig. 4 Temperature dependence of (A) ΔS_{ads} and (B) ΔH_{ads} for various MPs.

Our results also show that the magnitude[49] of ΔH_{ads} is representative of weak binding or physisorption for these particles. No strong chemical bonds are formed. van der Waals, Coulombic, hydration, hydrophobic and steric forces are involved. Accordingly, the ΔH_{ads} values reflect energetics of multiple steps including desorption of the displaced molecule, and its interaction with the adsorbed species. Fig. 4(B) clearly demonstrates that there is a difference in the ΔH_{ads} values with particles of different surface functional groups. For example, we find adsorption onto PSC particles containing carboxyl groups to be most exothermic. This is likely due to charge complexation and H-bonding with quaternary amine on DSMPI and the interfacial carboxylate ion. For PSS and PSC, ΔH_{ads} is relatively unchanged with temperature. On the other hand, PS and PSAA show a strong variation in ΔH_{ads} with temperature. For these particles, adsorption of DSMPI is endothermic below 35 °C, but becomes exothermic at higher temperature. A possible explanation is that at a higher temperature more polymeric chains are exposed, resulting in a greater occurrence of van der Waals interaction. It is also possible that additional functional groups, originally embedded, become exposed upon protrusion of the polymer chains, resulting in newly available binding sites.

From these observations, it can be surmised that despite the weak interaction, the MP interfacial functional groups do influence the binding strength. The variations in the thermodynamic parameters further imply that the MP/aqueous interface does not only accommodate different types of interactions

Table 1 Thermodynamic parameters of DSMPI adsorption at 22 °C. Uncertainties are based on 90% confidence interval of the fit function

	Thermodynamic parameters@22 °C		
Particles	ΔG_{ads} (kJ mol^{-1})	ΔS_{ads} (J K^{-1} mol^{-1})	ΔH_{ads} (kJ mol^{-1})
PS	−43.5 ± 2.0	165 ± 6	5.3 ± 0.2
PSS	−43.0 ± 1.5	131 ± 5	−4.4 ± 2.1
PSC	−40.2 ± 0.4	34.2 ± 0.4	−30.1 ± 0.3
PSAA	−35.5 ± 0.3	179 ± 2	17.2 ± 0.2

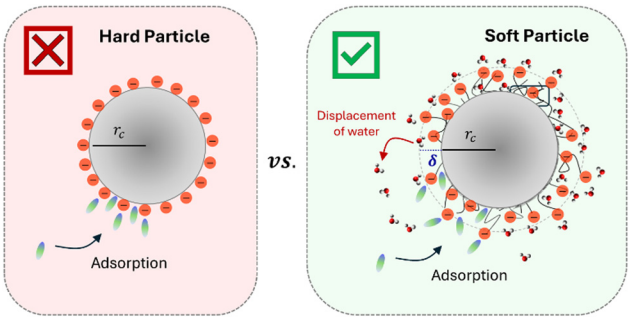

Fig. 5 Schematic of adsorption processes onto hard *vs.* soft colloidal/aqueous interfaces.

but is also dynamic, as is expected for a soft particle containing a charged polymer layer. This polymeric interfacial structure is prone to compression or expansion with temperature. The alteration in this interfacial layer with temperature can give rise to different types of interactions, which manifests in temperature dependent ΔS_{ads} and ΔH_{ads}. Existence of a ''hairy layer'' or a thick polymer structure of ~4–7 nm for polystyrene latex particles has been reported in the past.[50,51] The variation in the thermodynamic parameters observed is in sync with the notion of a polymer layer existing at the MP/aqueous interface.

Conclusions

In this work we have studied the adsorption process of charged and neutral organic compounds onto model microplastics of various interfacial chemical compositions. Adsorption isotherms (Fig. 2) collected *in situ* show that the adsorption of small organic compounds is spontaneous when opposite charges are involved. We conclude that Coulombic attraction is important for molecular interaction with MNPs. Small charged-neutral, hydrophobic compounds do not show proclivity for the MP surface because the MP/aqueous interfacial region is substantially hydrated and therefore polar. Further investigation on the adsorption of positively charged DSMPI revealed that ΔS_{ads} and ΔH_{ads} are not independent of temperature. Putting all these together, we get the following picture: the aqueous/plastic interface is not representative of a smooth surface of a hard particle (Fig. 5). It includes a soft polyelectrolyte layer of fixed charge density. Within this layer, water molecules are adsorbed. Fig. 5 distinguishes hard and soft colloids and the adsorption processes pertinent to these interfaces.

Our study highlights that adsorption of small organic compounds at the MP interface involves an exchange process and is representative of physisorption. Due to the release or displacement of water molecules, the sign of ΔS_{ads} is positive. That is adsorption is entropically driven. ΔH_{ads} also show dependency on the interfacial functional groups. Moreover, it bears the signature of multiple interactions, particularly for hydrophobic PS and mixed-charged interface of PSAA. That is, the adsorbate molecule is interacting with different regions at these interfaces. For interfaces with considerable charge density or with the potential for H-bonding, one type of interaction dominates. As a result, ΔH_{ads} is relatively constant with respect to temperature for PSC and PSS particles. As shown in Fig. 5, the polymeric layer in a soft particle is susceptible to movement and alteration with temperature. This exposes different interaction sites and modifies the distribution of water molecules in the polyelectrolyte layer. As a result, the nonlinear variation of ΔG_{ads} with temperature (Fig. 3) is a manifestation of the soft interfacial characteristic of MNPs.

In conclusion, the interfacial composition of micro- and nano-plastics in contact with water is complex. Molecular adsorption onto MNP interfaces may entail a wide range of forces. This study narrows down some of these driving forces and it highlights the significance of soft interfacial structure on molecular adsorption. Not only Coulombic attraction but hydrated polymer layer influences adsorption affinity. Thus, in addition to adapting a colloidal view of plastic particles, considering their soft polymeric interfacial structure for molecular adsorption is important. Within the aquatic environment, MNPs are subject to various factors such as photochemical aging and fouling. These processes are likely to change their interfacial structure. The impact of these factors on molecular adsorption remains to be explored; however, the present study on pristine particles provides a foundation for the future investigations to come.

Author contributions

Ikechukwu Kanu: data curation, formal analysis, investigation, validation; Amrit Ojha: data curation, formal analysis, investigation, validation; Kalie Adams: formal analysis, investigation, validation; Jacob Brooks: formal analysis, investigation, validation; Mahamud Subir: conceptualization, data curation, formal analysis, funding acquisition, investigation, methodology, project administration, resources, supervision, visualization, writing – original draft, writing – review & editing.

Conflicts of interest

There are no conflicts to declare.

Data availability

Supplementary information available: UV-Vis spectra of the SHG dye molecules, SHG-based adsorption isotherms, fit parameters of the polynomial function, Langmuir fit parameters of adsorption isotherms, and thermodynamic adsorption parameters. See DOI: **https://doi.org/10.1039/d5sm00488h**

Replicates of adsorption isotherm data and analyses supporting this article have been included as part of the SI. The SI also includes fitting parameters, residuals and associated error bars. The raw data in a spreadsheet format can be made available upon request.

Acknowledgements

This material is based upon work supported by the National Science Foundation under Grant No. 2304814.

Notes and references

1 T. K. Dey, M. E. Uddin and M. Jamal, Detection and removal of microplastics in wastewater: evolution and impact, *Environ. Sci. Pollut. Res.*, 2021, **28**(14), 16925–16947.

2 A. Alfaro-Núñez, D. Astorga, L. Cáceres-Farías, L. Bastidas, C. Soto Villegas, K. Macay and J. H. Christensen, Microplastic pollution in seawater and marine organisms across the Tropical Eastern Pacific and Galápagos, *Sci. Rep.*, 2021, **11**(1), 6424.

3 Y. Picó and D. Barceló, Analysis and Prevention of Microplastics Pollution in Water: Current Perspectives and Future Directions, *ACS Omega*, 2019, **4**(4), 6709–6719.

4 L. C. M. Lebreton, J. van der Zwet, J.-W. Damsteeg, B. Slat, A. Andrady and J. Reisser, River plastic emissions to the world's oceans, *Nat. Commun.*, 2017, **8**(1), 15611.

5 R. W. Chia, J.-Y. Lee, H. Kim and J. Jang, Microplastic pollution in soil and groundwater: a review, *Environ. Chem. Lett.*, 2021, **19**, 4211.

6 S. Lambert and M. Wagner, Microplastics Are Contaminants of Emerging Concern in Freshwater Environments: An Overview, in *Freshwater Microplastics: Emerging Environmental Contaminants?*, ed. M. Wagner and S. Lambert, Springer International Publishing, Cham, 2018, pp. 1–23.

7 Z. Tian, K. T. Peter, A. D. Gipe, H. Zhao, F. Hou, D. A. Wark, T. Khangaonkar, E. P. Kolodziej and C. A. James, Suspect and Nontarget Screening for Contaminants of Emerging Concern in an Urban Estuary, *Environ. Sci. Technol.*, 2020, **54**(2), 889–901.

8 J. P. G. L. Frias and R. Nash, Microplastics: Finding a consensus on the definition, *Mar. Pollut. Bull.*, 2019, **138**, 145–147.

9 C. Rochman; A. Andrady; S. Dudas; J. Fabres; F. Galgani; D. Lead; V. Hidalgo-Ruz; S. Hong; P. Kershaw; L. Lebreton; A. Lusher; R. Narayan; S. Pahl; J. Potemra; C. Rochman; S. Sherif; J. Seager; W. Shim; P. Sobral and L. Amaral-Zettler, *Sources, fate and effects of microplastics in the marine environment: Part 2 of a global assessment*, 2016.

10 O. D. Agboola and N. U. Benson, Physisorption and Chemisorption Mechanisms Influencing Micro (Nano) Plastics-Organic Chemical Contaminants Interactions: A Review, *Front. Environ. Sci.*, 2021, **9**, 678574.

11 T. Atugoda, M. Vithanage, H. Wijesekara, N. Bolan, A. K. Sarmah, M. S. Bank, S. You and Y. S. Ok, Interactions between microplastics, pharmaceuticals and personal care products: Implications for vector transport, *Environ. Int.*, 2021, **149**, 106367.

12 A. Al Harraq and B. Bharti, Microplastics through the Lens of Colloid Science, *ACS Environ. Au*, 2022, **2**(1), 3–10.

13 I. B. Gomes, J.-Y. Maillard, L. C. Simões and M. Simões, Emerging contaminants affect the microbiome of water systems—strategies for their mitigation, *npj Clean Water*, 2020, **3**(1), 39.

14 C. G. Daughton, Pharmaceutical Ingredients in Drinking Water: Overview of Occurrence and Significance of Human Exposure, *Contaminants of Emerging Concern in the Environment: Ecological and Human Health Considerations*, American Chemical Society, 2010, vol. 1048, pp. 9–68.

15 H. Ramírez-Malule, D. H. Quiñones-Murillo and D. Manotas-Duque, Emerging contaminants as global environmental hazards. A bibliometric analysis, *Emerging Contam.*, 2020, **6**, 179–193.

16 T. Rasheed, M. Bilal, F. Nabeel, M. Adeel and H. M. N. Iqbal, Environmentally-related contaminants of high concern: Potential sources and analytical modalities for detection, quantification, and treatment, *Environ. Int.*, 2019, **122**, 52–66.

17 E. P. Kolodziej and D. L. Sedlak, Rangeland Grazing as a Source of Steroid Hormones to Surface Waters, *Environ. Sci. Technol.*, 2007, **41**(10), 3514–3520.

18 L. Fu, J. Li, G. Wang, Y. Luan and W. Dai, Adsorption behavior of organic pollutants on microplastics, *Ecotoxicol. Environ. Saf.*, 2021, **217**, 112207.

19 E. Costigan, A. Collins, M. D. Hatinoglu, K. Bhagat, J. MacRae, F. Perreault and O. Apul, Adsorption of organic pollutants by microplastics: Overview of a dissonant literature, *J. Hazard. Mater. Adv.*, 2022, **6**, 100091.

20 S. H. Joo, Y. Liang, M. Kim, J. Byun and H. Choi, Microplastics with adsorbed contaminants: Mechanisms and Treatment, *Environ. Challenges*, 2021, **3**, 100042.

21 J. Dong, L. Li, Q. Liu, M. Yang, Z. Gao, P. Qian, K. Gao and X. Deng, Interactive effects of polymethyl methacrylate (PMMA) microplastics and salinity variation on a marine diatom Phaeodactylum tricornutum, *Chemosphere*, 2022, **289**, 133240.

22 S. A. Siddiqui, S. Singh, N. A. Bahmid, D. J. H. Shyu, R. Domínguez, J. M. Lorenzo, J. A. M. Pereira and J. S. Câmara, Polystyrene microplastic particles in the food chain: Characteristics and toxicity – A review, *Sci. Total Environ.*, 2023, **892**, 164531.

23 G. Mahadevan and S. Valiyaveettil, Understanding the interactions of poly(methyl methacrylate) and poly(vinyl chloride) nanoparticles with BHK-21 cell line, *Sci. Rep.*, 2021, **11**(1), 2089.

24 J. Hwang, D. Choi, S. Han, S. Y. Jung, J. Choi and J. Hong, Potential toxicity of polystyrene microplastic particles, *Sci. Rep.*, 2020, **10**(1), 7391.

25 C. C. Cheang, Y. Ma and L. Fok, Occurrence and Composition of Microplastics in the Seabed Sediments of the Coral Communities in Proximity of a Metropolitan Area, *Int. J. Environ. Res. Public Health*, 2018, **15**, 2270.

26 A. Rossatto, M. Z. F. Arlindo, M. S. de Morais, T. D. de Souza and C. S. Ogrodowski, Microplastics in aquatic systems: A review of occurrence, monitoring and potential environmental risks, *Environ. Adv.*, 2023, **13**, 100396.

27 J. Singh Jadaun, S. Bansal, A. Sonthalia, A. K. Rai and S. P. Singh, Biodegradation of plastics for sustainable environment, *Bioresour. Technol.*, 2022, **347**, 126697.

28 Q. Abbas, B. Yousaf, Amina, M. U. Ali, M. A. M. Munir, A. El-Naggar, J. Rinklebe and M. Naushad, Transformation pathways and fate of engineered nanoparticles (ENPs) in distinct interactive environmental compartments: A review, *Environ. Int.*, 2020, **138**, 105646.

29 F. G. Calvo-Flores; J. Isac-Garcéa and J. A. Dobado, Therapeutic Classes of PCs in the Environment. *Emerging Pollutants: Origin, Structure and Properties*, 2018, pp. 103–166.
30 R. W. Boyd, *Nonlinear Optics*, Academic Press, San Diego, 2nd edn, 2003.
31 Y. R. Shen, *The Principles of Nonlinear Optics*, John Wiley & Sons, Inc, Hoboken, 2003.
32 R. J. Sara, D. Coers, C. Behrman, J. Bobay and M. Subir, Molecular Adsorption and Physicochemical Properties at Liquid/Liquid Nanoemulsion Soft Interfaces: Effect of Charge and Hydrophobicity, *J. Phys. Chem. B*, 2024, **128**(12), 3004–3015.
33 M. Subir and Y. Rao, Environmental Interfacial Spectroscopy, *ACS In Focus* [Online], American Chemical Society, 2021, p. 1. , DOI: **10.1021/acsinfocus.7e5016**.
34 T. A. Williams, J. Lee, C. A. Diemler and M. Subir, Magnetic vs. non-magnetic colloids – A comparative adsorption study to quantify the effect of dye-induced aggregation on the binding affinity of an organic dye, *J. Colloid Interface Sci.*, 2016, **481**, 20–27.
35 M. Subir, J. Liu and K. B. Eisenthal, Protonation at the Aqueous Interface of Polymer Nanoparticles with Second Harmonic Generation, *J. Phys. Chem. C*, 2008, **112**(40), 15809–15812.
36 E. Poli, K. H. Jong and A. Hassanali, Charge transfer as a ubiquitous mechanism in determining the negative charge at hydrophobic interfaces, *Nat. Commun.*, 2020, **11**(1), 901.
37 P. Zhang, M. Feng and X. Xu, Double-Layer Distribution of Hydronium and Hydroxide Ions in the Air-Water Interface, *ACS Phys. Chem. Au*, 2024, **4**(4), 336–346.
38 R. J. Saykally, Two sides of the acid–base story, *Nat. Chem.*, 2013, **5**(2), 82–84.
39 L. S. McCarty and G. M. Whitesides, Electrostatic Charging Due to Separation of Ions at Interfaces: Contact Electrification of Ionic Electrets, *Angew. Chem., Int. Ed.*, 2008, **47**(12), 2188–2207.
40 D. Myers, *Surfaces, interfaces, and colloids*, Wiley, New York, 1999, vol. 415.
41 M. Subir and Y. Rao, *Environmental Interfacial Spectroscopy*, American Chemical Society, 2021, p. 1.
42 L. Kaylor, P. Skelly, M. Alsarrani and M. Subir, Enhanced malachite green photolysis at the colloidal-aqueous interface, *Chemosphere*, 2022, **287**, 131953.
43 K. Sahu, K. B. Eisenthal and V. F. McNeill, Competitive Adsorption at the Air–Water Interface: A Second Harmonic Generation Study, *J. Phys. Chem. C*, 2011, **115**(19), 9701–9705.
44 U. Gaur and B. Wunderlich, Heat Capacity and Other Thermodynamic Properties of Linear Macromolecules. V. Polystyrene, *J. Phys. Chem. Ref. Data*, 1982, **11**(2), 313–325.
45 M. Tanase, A. Soare, V. David and S. C. Moldoveanu, Sources of Nonlinear van't Hoff Temperature Dependence in High-Performance Liquid Chromatography, *ACS Omega*, 2019, **4**(22), 19808–19817.
46 S. Kishani, T. Benselfelt, L. Wågberg and J. Wohlert, Entropy drives the adsorption of xyloglucan to cellulose surfaces – A molecular dynamics study, *J. Colloid Interface Sci.*, 2021, **588**, 485–493.
47 J. Fu and J. B. Schlenoff, Driving Forces for Oppositely Charged Polyion Association in Aqueous Solutions: Enthalpic, Entropic, but Not Electrostatic, *J. Am. Chem. Soc.*, 2016, **138**(3), 980–990.
48 E. Nishiyama, M. Yokota and I. Tsukushi, Analysis of the configurational heat capacity of polystyrene and its monomer and oligomer above the glass transition temperature, *Polym. J.*, 2022, **54**(1), 33–39.
49 H.-J. Butt; K. Graf and M. Kappl, *Physics and Chemistry of Interfaces*, Wiley-VCH, Weinheim, 2006.
50 Z. F. M. Said, Possible evidence for the existence of a hairy layer at the surface of polymer latex particles, *Polym. Int.*, 1998, **47**(4), 459–464.
51 J. E. Seebergh and J. C. Berg, Evidence of a hairy layer at the surface of polystyrene latex particles, *Colloids Surf., A*, 1995, **100**, 139–153.

